Mechanical effects analysis of inverted arch

IOP Conf. Series: Materials Science and Engineering **490** (2019) 032026 doi:10.1088/1757-899X/490/3/032026

Mechanical effects analysis of inverted arch

Yueduo Fang[1], Kewei Ding[2,*]

[1]Anhui Electric Power Transmission and Transformation Co., Ltd., Hefei , China
[2]Civil engineering school, Anhui Jianzhu University, Heifei, China

*Corresponding author e-mail: 2764060693@qq.com

Abstract: In order to study the mechanical effect of the inverted arch of the expansive soil layer, Midas, one kind of finite element analysis software, was used to simulate the support forms of the two tunnels, the vertical displacement, the vertical stress, the shear stress, the distribution of the plastic zone of tunnel surrounding rock and the stress of the lining are compared and analyzed. The results show that the integrity of inverted arch tunnel is relatively good, which can effectively restrain the bottom deformation, reduce the compressive stress at the arch shoulder and arch foot, and control The plastic zone of the surrounding rock, and can better improve the overall mechanical property of the lining structure, and by analyzing the best inverted arch radius to find the most reasonable radius value.

1. Introduction

Being an inverted arch structure set at the bottom to improve stress conditions of the tunnel's lining structure, the inverted arch is an important part of the tunnel lining structure [1]. The role of the inverted arch is more obvious especially in weak surrounding rocks with a larger lateral pressure coefficient, or surrounding rocks with a large horizontal tectonic stress or with conspicuous flowing deformation, or swelling rocks [2]. On the one hand, the inverted arch needs to effectively transfer the tunnel's upper stratum pressure and the pavement load to the ground. On the other hand, it should resist against the counter-force from the tunnel's lower stratum. Thus, a proper setting of the inverted arch can effectively control the deformation range and influence scope of the tunnel surrounding rock, improve the form of stress on the lining structure, and coordinate the axial force and bending moment distribution of the lining structure [13]. In primary lining of the tunnel, the inverted arch can not only reduce settlement deformation caused by inadequate bearing capacity of the tunnel foundation, but also prevent the heaving floor from swelling deformation and adjust the role of the lining stress [3]. Wang et al. studied mechanical behaviors of the tunnel inverted arch by combining the large-scale model experiment with the infinite analysis [4]. Results suggest that the tunnel inverted arch is essential to improve the bearing capacity of the tunnel structure, restrain the internal plastic zone of the surrounding rock and the displacement around the tunnel from further expansion, and promote safety of the lining structure [5].

When the geographical conditions are poor, the excavation length of the inverted arch should not exceed 5 m ～ 10 m[12]. That primary lining connects form a loop can prevent the surrounding rock from major deformations, and enhance lining of the arch shoulder and arch foot. Meanwhile, inverted arch setting can, to a large extent, promote the stress status of the tunnel structure, avoid internal crowdedness to cause shear failure, and contribute to stability of the tunnel structure [14]. Therefore, the decisive role of the inverted arch in the tunnel's primary lining stress system cannot be ignored [3].

This paper is set against the engineering background of the bored tunnel in Hefei for the transfer stop between Line 2 and Line 3, where Changjiang West Road and Qianshan Road converges. MIDAS,

one kind of finite element analysis software, is used to comparatively analyze mechanical effects of two tunnels—one with the inverted arch and the other without the inverted arch. It is hoped that research findings of this paper can provide references for construction of the tunnel inverted arch in typical areas such as with swelling soil.

2. Engineering background

Qianshan Road Stop of Hefei Subway Line 2 is located in the interaction between Changjiang West Road and Qianshan Road. It is a transfer stop from Line 2 to Line 3 or vice versa. Line 2 has its stop paved along Changjiang West Road, constituting an underground three-floor island-type stop, while Line 3 has its stop extended along Qianshan Road, featuring an underground two-floor island-type stop. The affiliated No. 1 Entrance is in the northeast quadrant of the interaction, and is a structure in the first floor underground. Through underground excavation, the stop of Line 2 and the stop of Line 3 are connected. The covering depth of the bored tunnel connecting Line 3 is 5m, which mainly consists of 3m thick artificial filling soil and 2m thick clay. The major part of the cave body is made up of 1.8m thick clay and 2.8m thick fully-weathered argillaceous sandstone. The bottom plate is located on the deeply-weathered argillaceous sandstone.

3. Establishment of the calculation model

Solid elements are used to simulate the tunnel surrounding rock and the soil mass. The surrounding rock and the soil mass are both regarded as isotropic and continuous elastoplastic materials consisting the elastoplastic constitutive relation based on the Mohr-Coulomb criterion [6]. Both the primary lining and the secondary lining are simulated using plate elements. The physical mechanical parameters (including the elasticity modulus E, the cohesive stress c and the internal friction angle ϕ)of the soil layer in the reinforced area are moderately increased to approximately simulate reinforcement effect of the pipe roof and the advanced small duct pre-grouting on the stratum. The elasticity modulus of the steel arch is converted into the elasticity modulus for shotcreting of the reinforced stratum [4]. The passivation and activation functions of MIDAS are employed to simulate the dynamic process of excavation and lining in tunnel construction.

The model boundary is automatically restricted using MIDAS. Excluding the free surface, five of the six surfaces of the model has normal restriction imposed on them [7], and the self-weight load is adopted. Vertically, the model is set to be 15m, and has four kinds of soil layers, including miscellaneous fill, clay, fully-weathered argillaceous sandstone and heavily-weathered argillaceous sandstone. Horizontally, the model is set to be 40m; longitudinally, 30m. If there is an inverted arch, the inverted arch radius is set to be 16m. The calculation model, based on the above settings, is presented in Fig. 1. Physical mechanical parameters of the surrounding rock and the lining structure adopted by the model in this paper are usual.

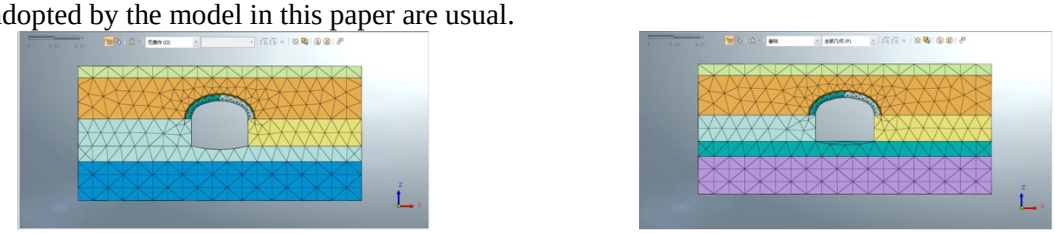

(a) Tunnel model with the inverted arch (b) Tunnel model without the inverted arch

Figure 1. Calculation model

4. Numerical simulation analysis

4.1 Analysis of the soil body vertical displacement

During the excavation and lining process of the tunnel, the surrounding rock will unavoidably suffer different degrees of disturbance and damage, thus causing changes of the displacement field [15]. As

one observes displacement nephogram in Fig. 2, the vertical surrounding rock displacement of the two models is both reflected as subsidence in the vault part, protruding of the bottom part and expansion to the surrounding of the cave in side walls.

After tunnel excavation is finished, the maximum subsidence value of Model 1 (the tunnel model without the inverted arch) and Model 2 (the tunnel model with the inverted arch) is found within the scope of the vault. The maximum vertical displacement of the two models is 20.071mm and 19.776mm, respectively. The maximum subsidence value of Model 2 is smaller than that of Model 1 by 1.470%. The maximum vertical protruding value of the surrounding rock at the tunnel bottom is 10.640mm and 7.940mm in Model 1 and Model 2, respectively. Comparatively, the maximum vertical protruding value of Model 2 is smaller than that of Model 1 by 25.376%. Benefiting from the integral tunnel structure constituted by the inverted arch and the cave lining, the integrity of the tunnel lining structure is strengthened to better resist against protruding deformation of the surrounding rock at the bottom of the tunnel [8]. However, the role of the inverted arch in resisting against deformation of the tunnel vault is not obvious. This suggests that a main advantage of the inverted arch is to curb deformation of the tunnel bottom.

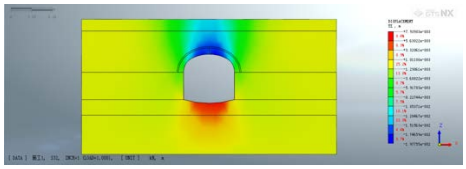

(a) Vertical displacement nephogram of the tunnel model without an inverted arch

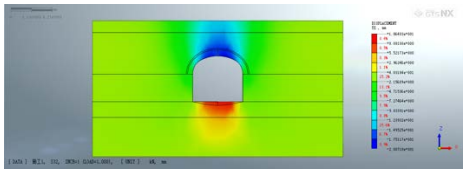

(b) Vertical displacement nephogram of the tunnel model with an inverted arch

Figure 2. Vertical displacement nephogram of Model 1 and Model 2

4.2 Analysis of the soil body vertical stress

The vertical stress nephogram of the tunnel are shown in Fig. 3. It can be seen that the vertical stress distribution rules of the two models are similar to each other. The tunnel structure is mostly under stress. Only the arch vault and the arch bottom are under tension. The major parts under stress include the arch shoulder and the arch foot. The maximum stress of the two tunnel models both occurs at the arch shoulder, which is 0.298MPa and 0.256MPa, respectively. In other words, the maximum stress of the tunnel model with an inverted arch (Model 2) is 14.1% smaller than that without an inverted tunnel (Model 1). The maximum stress at the arch bottom of both models changes dramatically, dropping to 0.183MPa and 0.149MPa, respectively, in which Model 2 is 18.5% smaller than Model 1. The arch vault tensile stress of Model 2 at the arch vault is 0.062MPa, which is 5.8% smaller than that of Model 1 or the tunnel model without an inverted arch. This means that the inverted arch structure can significantly reduce the vertical compressive stress on the arch shoulder and the arch foot of the tunnel, but its effect on alleviating the vertical compressive stress in the arch vault is not obvious. Therefore, the role of the inverted arch in reducing stress is relatively significant at the arch shoulder and the arch foot.

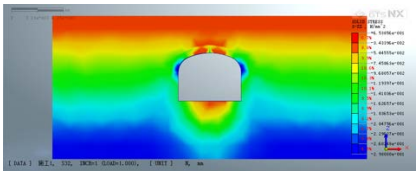

(a) Vertical stress nephogram of the tunnel model with the inverted arch

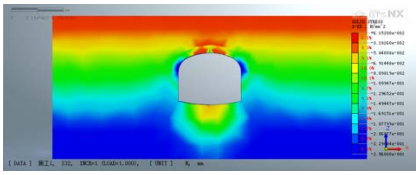

(b) Vertical stress nephogram of the tunnel model without the inverted arch

Figure 3. Vertical stress nephogram of Model 1 and Model 2

4.3 Analysis of the soil body shear stress and plastic zone

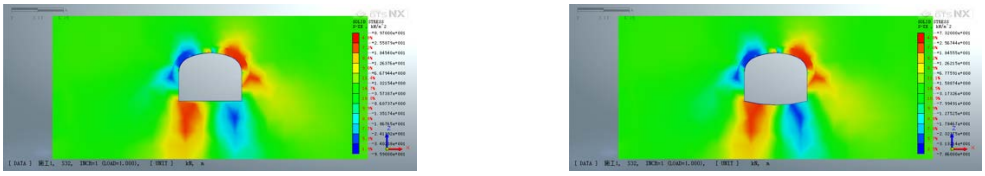

(a) Shear stress nephogram of the tunnel model without the inverted arch

(b) Shear stress nephogram of the tunnel model with the inverted arch

Figure 4. Tunnel shear stress nephogram of Model 1 and Model 2

(a) Schematic diagram of the plastic zone of the tunnel model without the inverted arch

(b) Schematic diagram of the plastic zone of the tunnel model with the inverted arch

Figure 5. Schematic diagram of the tunnel plastic zone

From Fig. 4, it can be observed that the surrounding rock shear stress of the two tunnel models both features an X-shaped distribution, and is bilaterally symmetric revolving around the perpendicular plane of the tunnel. Besides, the shear stress only distributes near the cave entrance, and is relatively large on four corners of the tunnel. Table 1 compares the shear stress value and changes at four corners of the two models. From Table 1, it can be noticed that the maximum shear stress of Cross-Section 1 both appears at the left arch foot of the two models, and that the shear stress of the two arch feet is about twice as much as that of the arch.

Tunnel excavation can result in shear failure of the surrounding rock. As shown in Fig. 5, the surrounding rock shear failure zone (namely the plastic zone) is mainly located at four corners of the tunnel. Especially on two sides of the arch bottom, the shear failure zone radiates from the tunnel center to form a "Λ" shape. The shear stress at the arch foot is huge, so the shear failure zone on two sides of the arch bottom is relatively large. The surrounding rock plastic zone of the tunnel shows similar distribution rules in the two models. One difference is that the plastic zone at the arch foot of Model 2 decreases significantly. This is because the arch-shaped connection part between the inverted arch and the side wall alleviates concentration of the surrounding rock stress at the arch foot [10]. This finding substantiates that the inverted arch lining structure plays an important role in reducing the surrounding rock shear failure zone.

4.4 Analysis of the inverted arch radius

The minimum inverted arch radius of the two models is set to be $R_2 \geq 2R_1$ (R_1=6.5, the arch vault radius). In order to study influence of the inverted arch radius on the tunnel's overall structure, the tunnel's inverted arch radius of the two models is comparatively analyzed. Seven inverted arch radiuses are chosen to analyze the vault subsidence, the arch bottom protruding and the cave surrounding convergence value with R_2 ranging from 13m to 19m. See Fig. 6, Fig. 7 and Fig. 8.

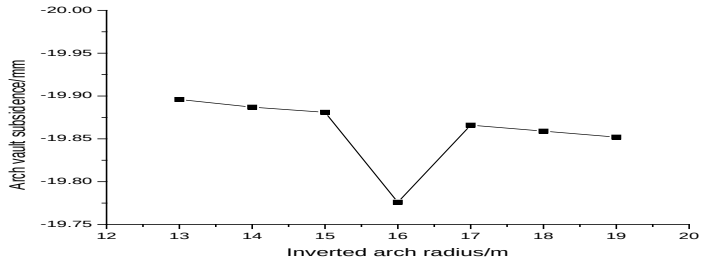

Figure 6. Arch vault subsidence displacement curve under different inverted arch radiuses

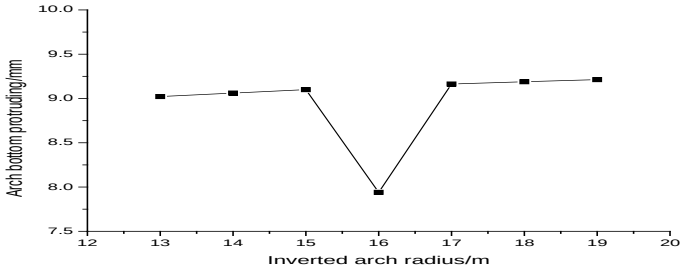

Figure 7. Arch bottom protruding displacement curve under different arch radiuses

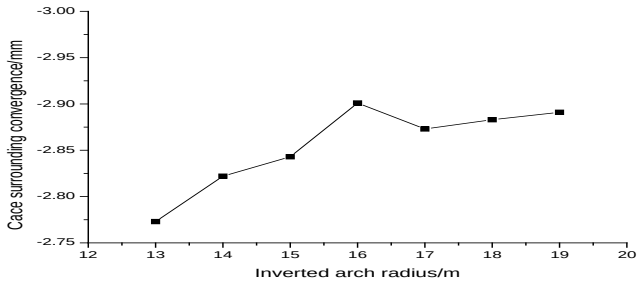

Figure 8. Cave surrounding convergence displacement curve under different arch radiuses

5. Conclusions

Based on the above analysis, this paper comes to the following conclusions:

(1) Based on contrastive analysis results of the two models, existence of the inverted arch has a huge influence on the maximum vertical protruding value of the tunnel bottom, but a slight influence on vertical subsidence of the tunnel vault. Benefiting from the favorable overall integrity of the inverted arch, the maximum vertical protruding value of the arch bottom is reduced by 25.376%.

(2) The vertical stress analysis of the tunnel suggests that the inverted arch can significantly reduce the vertical compressive stress on the tunnel's arch foot and arch shoulder, but the reduction effect on the vertical compressive stress on the arch vault is not obviously. Therefore, the inverted arch can only effectively alleviate stress on the arch shoulder and the arch foot.

(3) The surrounding rock shear stress of the two tunnel models forms an X-shaped distribution. Since the shear stress on two sides of the arch bottom is about twice as much as that of the arch vault sheer stress, the shear failure zone on two sides of the arch bottom is also larger. The surrounding rock plastic zone of the two models is both located at four corners of the tunnel cave. Meanwhile, the two sides of the tunnel bottom obviously radiate from the tunnel center to form an "Λ" radial pattern. The plastic zone at the arch foot of Model 2 is obviously smaller than that in Model 1. This means the inverted arch lining structure is essential to curb expansion of the surrounding rock shear failure zone.

(4) The inverted arch is an important part of the lining structure. The contrastive analysis of the lining stress of the two models shows that setting of the inverted arch can effectively improve the

stress distribution of the lining structure, and promote stress resistance of the lining structure. This provides evidence for the effect of the inverted arch on improving the overall stress resistance of the lining structure.

(5) The tunnel of Qianshan Road Stop of Line 2 for transfer between Line 2 and Line 3 features a tunnel without the inverted arch. Research findings in this paper show that, if the inverted arch can be set for the tunnel, the tunnel's overall stress resistance can be greatly improved. Nevertheless, the various stress parameters of the designed tunnel without the inverted arch can all reach the standard requirements. Thus, based on various economic concerns, the tunnel design without the inverted arch is adopted.

(6) Based on analysis of the vault subsidence, vault bottom protruding and tunnel's cave surrounding convergence of the two models, it can be seen that, when the inverted arch radius is set to be 16m, the influence of the inverted arch radius on the right arch waist, though whose crosswise displacement increases, is slight, but the influence on the arch vault subsidence and the arch bottom protruding is significant. Results also show that 16m is the optimal value of the inverted arch radius, which can contribute to the overall structural stability.

Acknowledgments

This work is supported by Key Laboratory Construction Project of Anhui Province (1501041133, AJ-CXY-KF-17-11).

References

[1] Yi D. Site monitoring and numerical simulation analysis of the highway tunnel IV1 surrounding rock inverted arch, Hebei University of Technology, 2012.
[2] Deng J. Renovation techniques of quality defects with inverted arches and bottom plates of the railway tunnel, Keiji, Economy and Market, 2014 (9): 11-12.
[3] Jiang T. H. Research into key techniques of the shallow crumbly strata tunnel construction, Chang'an University, 2012.
[4] Su J. C., Zhang Z. C., Gao Y., et al. Discussion of dabianshan mountainous highway multiple arch tunnel design, Tunnel Construction, 2004, 24 (3): 12-14.
[5] Fang Q. Structural response analysis under inverted arch tunnel in different construction methods, Technology & Economy in Areas of Communications, 2014, 16 (1): 12-16.
[6] Sun G. H., Cheng H. & Wang D. L. Comparative analysis and application of the shallow urban tunnel excavation plan, Journal of Anhui Jianzhu University, 2010, 18 (4): 42-46.
[7] Chen J. & Xiao D. J. Numerical simulation research of ground surface settlement caused by construction of tunnel with shallow depth excavation, Engineering Construction, 2012, 44 (2): 10-13.
[8] Li Y. M. Numerical simulation and ground deformation analysis of the adjacent building pit construction, Wuhan University of Technology, 2007.
[9] Liu Y. R. Tunnel support optimization design based on the inverted arch numerical analysis, Hebei University of Industry, 2007.
[10] Li M., Chen H. K & Ye S. Q. Numerical simulation of the highway tunnel inverted arch mechanical behaviors, National Highway Tunnel Academic Exchange Conference, 2007.
[11] Ye D. M., Huang Z. Y. & Zhang Q. J. Influence of the inverted arch on the lining structure stress, East China Highway, 2010 (3)： 61-64.
[12] Deng R. G. & Wang Y. H. Study on tunnel invert construction stability under grade Ⅳ surrounding rock condition, Shanxi Architecture, 2015, 41 (10): 167-169.
[13] Chen Y. Z. A technical research into mechanical characteristics and fast construction techniques of the highway tunnel inverted arch lining structure, China Academy of Railway Sciences, 2012.
[14] Wang M. N & Weng H. M. Study on the mechanic behavior of tunnel inverted arch, Chinese Journal of Geotechnical Engineering, 1996, 18 (1): 46-53.
[15] Meng D. L. Analysis of inverted arch optimization based on numerical simulation, Transportation Science & Technology, 2015 (4): 81-83.